津波探知レーダの研究状況調査

平成23年8月26日

電波航法研究会

渡辺康夫

講演内容

1. はじめに
2. 2004年12月26日のスマトラ沖津波と衛星搭載電波高度計
3. 2011年3月11日の東北太平洋沖地震の津波とHFレーダ
4. おわりに

発表の背景と目的

2004年12月26日，スマトラ･アンダマン地震発生の約2時間後，海洋観測衛星Jason-1とTOPEX/Poseidonがインド洋を伝播中の津波の第一波の上空を偶然通過し，電波高度計によってdeep oceanにおける津波波高のプロファイル及びレーダ後方散乱強度を初めて明瞭に計測した.

2011年3月11日，東北太平洋沖地震の約22時間後，津波を待ち受けていたチリのHFレーダが沿岸に接近する津波のocean surface currentを初めて計測した.

本発表では注目すべきこの二件を中心に，関連研究を含めて文献をサーベイした結果を報告する.

Table 1a Instrument Characteristics of Jason-1 altimeter (Poseidon-2)

Pulse repetition freq.	2060Hz±10%	
Pulse duration	105.6 μ s	
Pulse compression ratio	33600	
Integration time	50ms	
	Ku-band	C-band
Center frequency	13.575GHz	5.3GHz
Bandwidth	320MHz	320/100MHz
RF output power	38.3dBm	43.0dBm
Antenna gain	42.2dB	32.3dB
Tx pulse mode (nominal)	Interlace: 3Ku 1C 3Ku	

(G. Carayon et al., IGARSS-02, 2002)

Table 1b Example of measurement performances

	In flight data	Ground test	Require-ment
Mean SWH	2.18m	2.14m	
SWH 1s noise	14.7cm	13.1cm	20cm
Ku range 1s noise	1.7cm	2 cm	
C range 1s noise	3.6cm	5.3cm	
Dual freq. range 1s noise	1.8cm	2 cm	2.5cm

(G. Carayon et al., IGARSS-02, vol.2, 774-776, 2002)

Fig. 1. 2004 Indian Ocean tsunami propagation

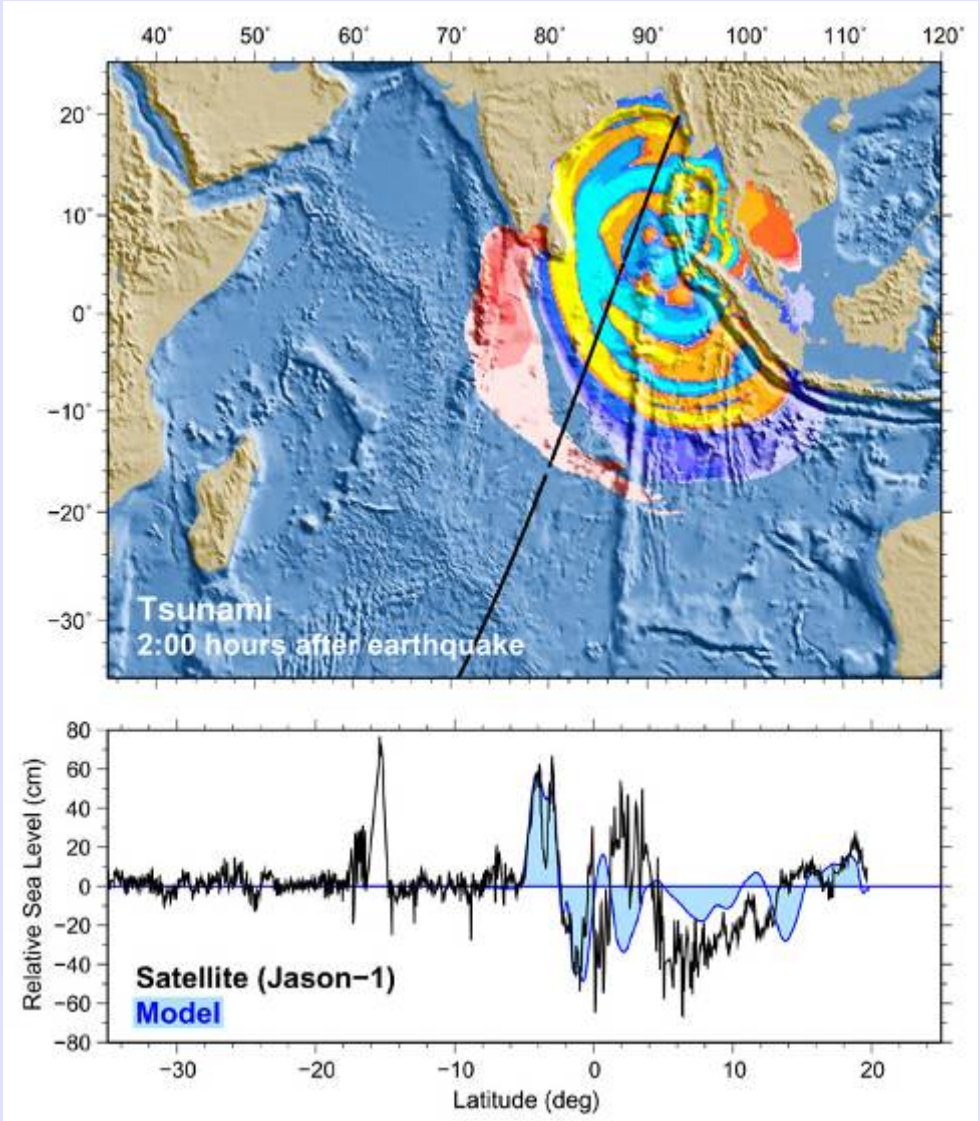

Measurement by Jason-1

(NOAA News Online, 10 January 2005: 2004 tsunami propagation)

Fig. 2 Sea surface height anomalies by Jason-1

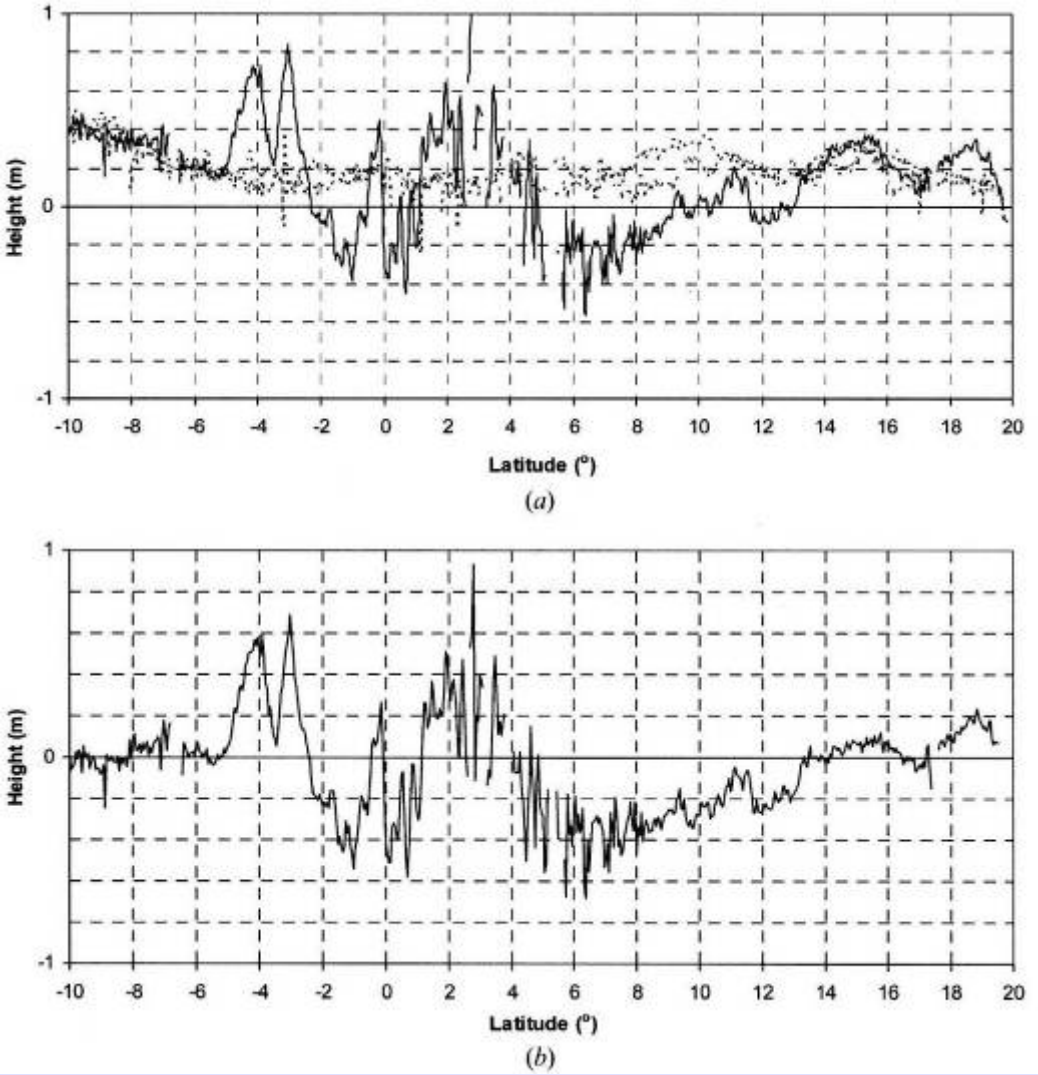

——— Cycle 109 (26 Dec. 2004)

····· Ave. of cycles 108, 110

Cycle 109 with the ave. subtracted

(J. Gower, Int. J. Remote Sensing, vol.28, Nos.13-14, 2829-2913, July 2007)

Fig. 3 Sea surface height anomalies: the measured and the theory for Jason-1

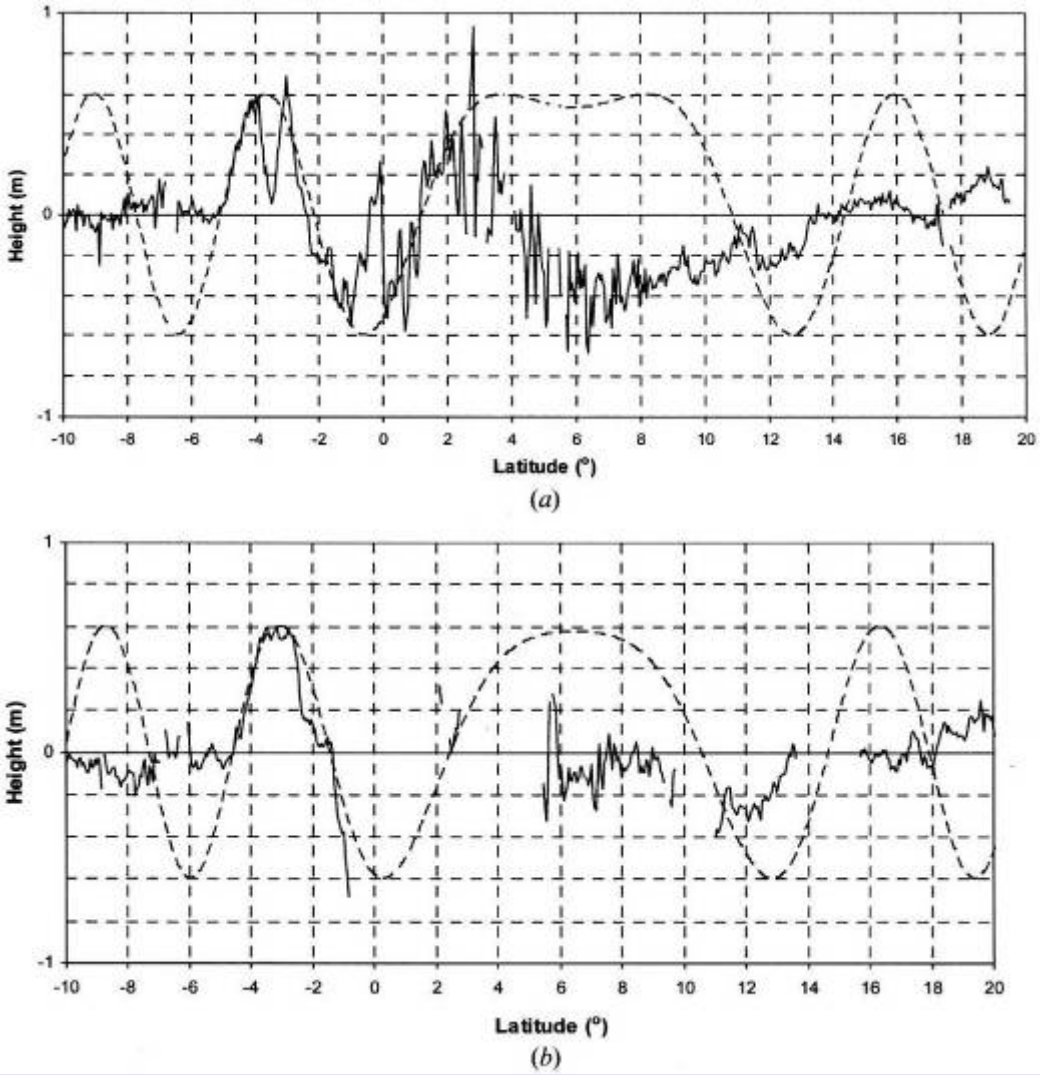

Corrected sea surface height on cycle 109

Model sine wave of wavelength 580km and amplitude 0.6m

Topex/Poseidon data as for (a)

(J. Gower, Int. J. Remote Sensing, vol.28, Nos.13-14, 2829-2913, July 2007)

Table 2 Six observations by the three altimeters

	Time UT	Lat. (º)	Lon. (º)	Time (s)	Distance (km)	Speed (km/h)	Av. Depth (m)
Epicenter	00:58:53	3.2	94.2				1530
Jason S	02:53:51	-4.56	84.12	6900	1415	739	4300
Jason N	02:59:53	13.15	90.56	7260	1240	615	2975
Topex S	03:00:34	-4.06	82.88	7300	1495	738	4280
Topex N	03:06:26	13.15	89.13	7650	1180	554	2415
Envisat S	04:19:24	-17.01	82.57	12030	2590	774	4715
Envisat N	04:09:18	18.93	90.65	11425	1795	565	2510

(J. Gower, Int. J. Remote Sensing, vol.28, Nos.13-14, 2829-2913), July 2007)

Fig. 4 Multisatellite Time-Spatial Interpolation

Proposed method

$$SLA_{ref}(\phi,\theta,t) = \Sigma(w_i \cdot SLA_{obs,i}) / \Sigma w_i \quad (1)$$

$$\Sigma w_i = \exp[-(r_i/R)^2 - (t_i/T)^2] \quad (2)$$

$$h_{tsunami}(\phi,\theta,t) = SLA_{obs}(\phi,\theta,t) - SLA_{ref}(\phi,\theta,t) \quad (3)$$

Conventional method

$$h_{tsunami}(\phi,\theta,t) = SLA_{obs}(\phi,\theta,t) - SLA_{obs}(\phi,\theta,t-c) \quad (4)$$

$SLA_{ref}(\phi,\theta,t)$: the defined reference height at the latitude ϕ, longitude θ, and date of a tsunami searching point.

SLA_{obs}: an anomaly in an observed sea surface height.

$h_{tsunami}$: the tsunami height.

r_i = the distance between the location of the ith datum and the tsunami searching point.

t_i = time difference of observations between a tsunami observation point (t) and the ith datum.

R, T = scale parameters, fixed at R = 45km and T = 10days.

(Y. Hayashi, J. Geophysical Research, vol. 113, C01001, 1/9-9/9, 2008)

Fig. 5 Profile of tsunami height extracted from Jason-1 data by Multisatellite Time-Spatial Interpolation method

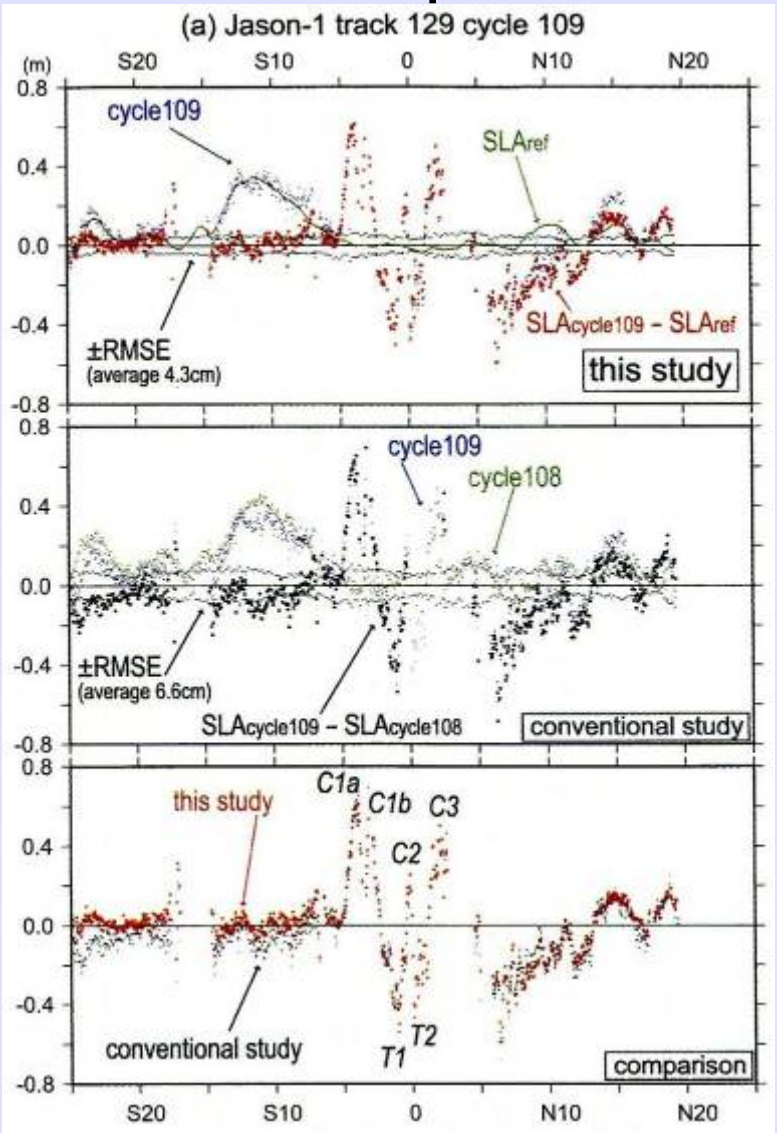

SLA: sea level anomaly

RMSE: root mean square residual errors

(Y. Hayashi, J. Geophysical Research, vol. 113, C01001, 1/9-9/9, 2008)

Table 3 Residual errors and number of valid points in defined tsunami height

Satellite	RMS residual error, cm		No. valid points		No. sampl. pts.
	Hayashi	Others	Hayashi	Others	
Jason-1	4.3	6.6	412	356	482
Topex/ Poseidon	4.9	6.5	285	88	490
Envisat	4.4	9.3	659	642	702
GFO (Track 208)	4.2	8.0	938	923	938
GFO (Track 210)	4.9	10.0	971	928	996

(Excerpt: Y. Hayashi, J. Geophysical Research, vol. 113, C01001, 2008)

Fig. 6 Tsunami shadows

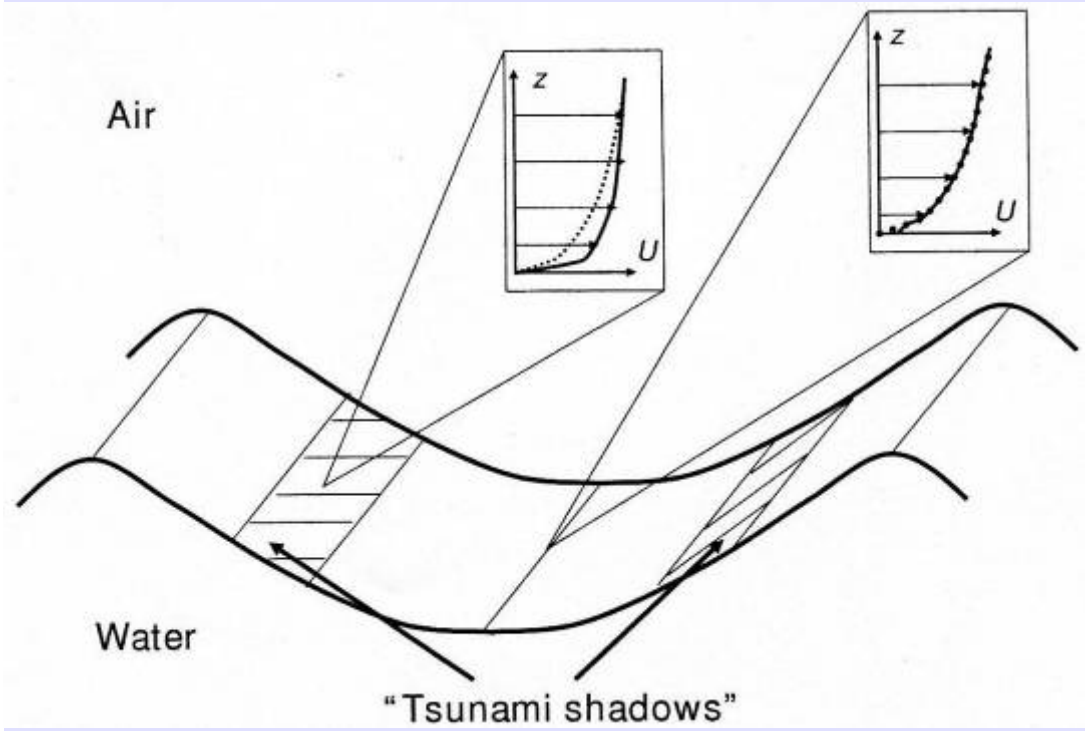

A conceptual representation of "tsunami shadows" and their theoretically predicted relation to the tsunami-induced wind velocity perturbations. "Tsunami shadows" (hatched) are parallel to the tsunami wave front and occur in between the tsunami troughs and crests where the wind perturbation is maximal. Perturbed (solid lines) and unperturbed (dotted lines) wind velocity is shown as a function of height above the ocean surface.

(O. A. Godin, J. Geophysical Research, vol. 109, C05002, 2004)

Fig. 7 Jason-1 data for pass 129 from 6º to 2ºS

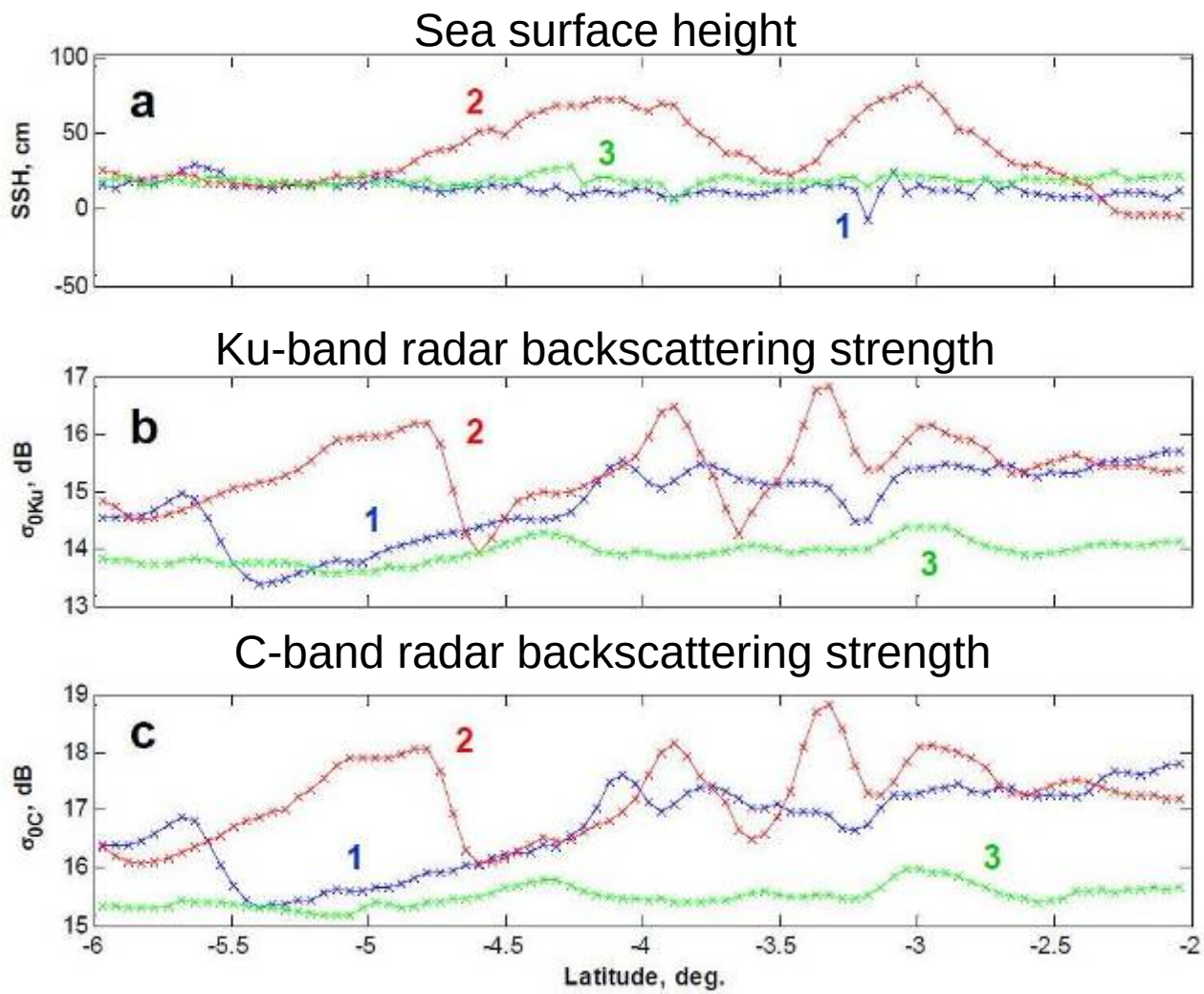

(1) Obtained days before
(2) coincident with cycle 109
(3) 10days after.

(O. A. Godin et al., Natural Hazards and Earth System Sciences, vol. 9, 1135-1147, 2009)

Fig. 8 A stylized shore line (bold) at the top and offshore bathymetry contours

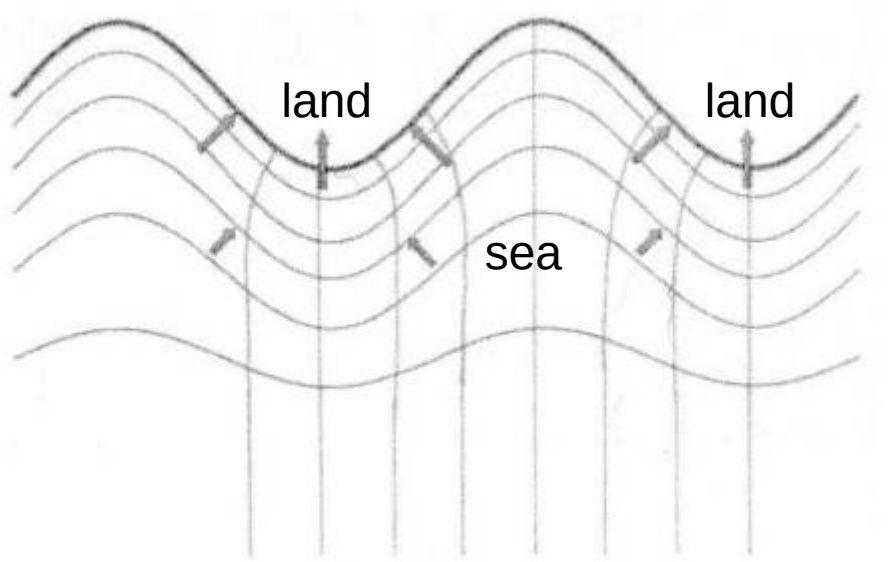

(a) refract swell energy and wind waves (entering the diagram along ray paths from bottom) onto the headlands and away from the bays

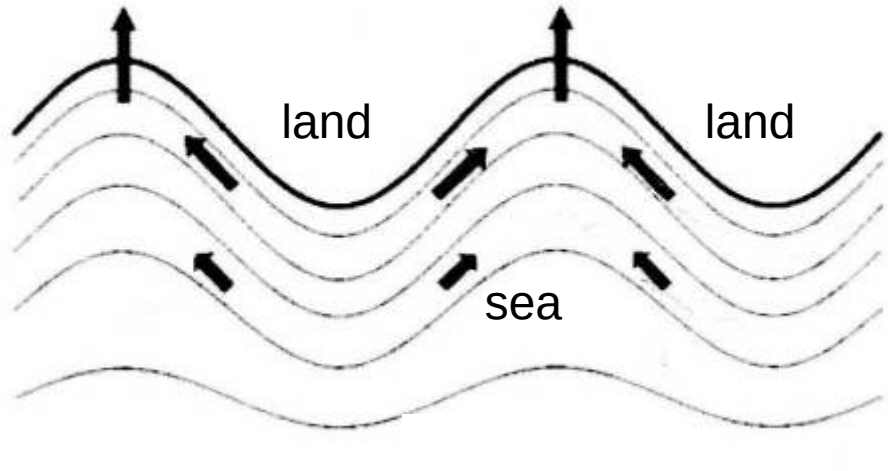

(b) direct the momentum in a tsunami along the bathymetry contours to give the most intense effects in the bays

(M. L. Heron et al., International Journal of Remote Sensing, vol. 29, No. 21, 6347-6359, 10 Nov. 2008)

Fig. 9 Model calculation for the impact of the 26 Dec. 2004 tsunami on the Seychelles

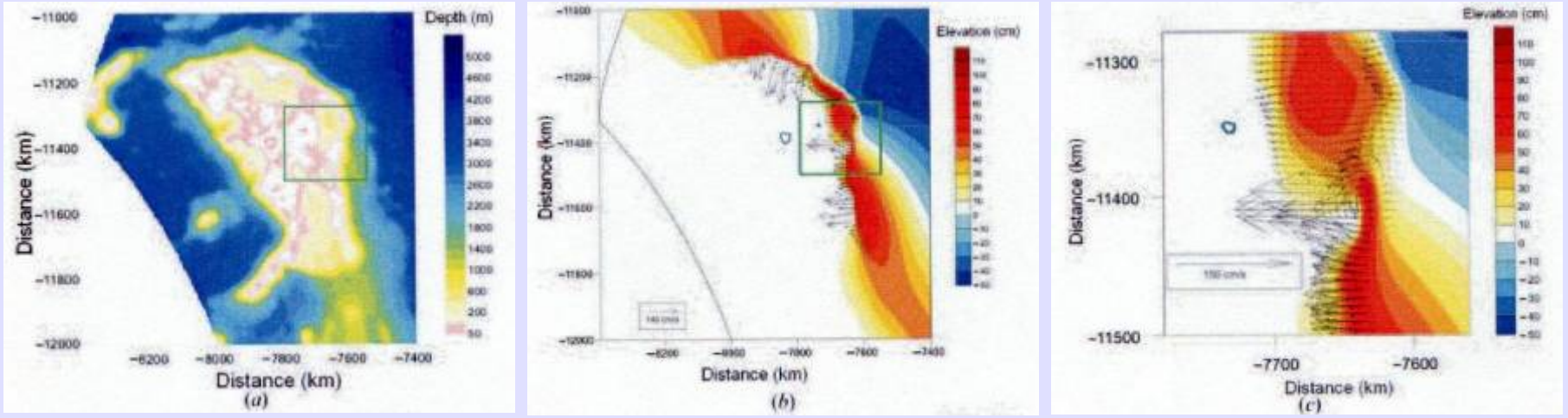

(a) the bathymetry around the Seychelles shows a platform in otherwise deep water,
(b) the large scale amplification of sea surface height (contours) and surface current (vectors) when the first tsunami wave encounters the edge of the continental shelf, and
(c) a section of the shelf-edge (corresponding to the box in (a) and (b)), which shows the area that could be monitored by a HF ocean radar.

(M. L. Heron et al., Int. J. Remote Sensing, vol. 29, No. 21, 6347-6359, 10 Nov. 2008)

Fig. 10 German Indonesian Tsunami Early Warning System (GITEWS)

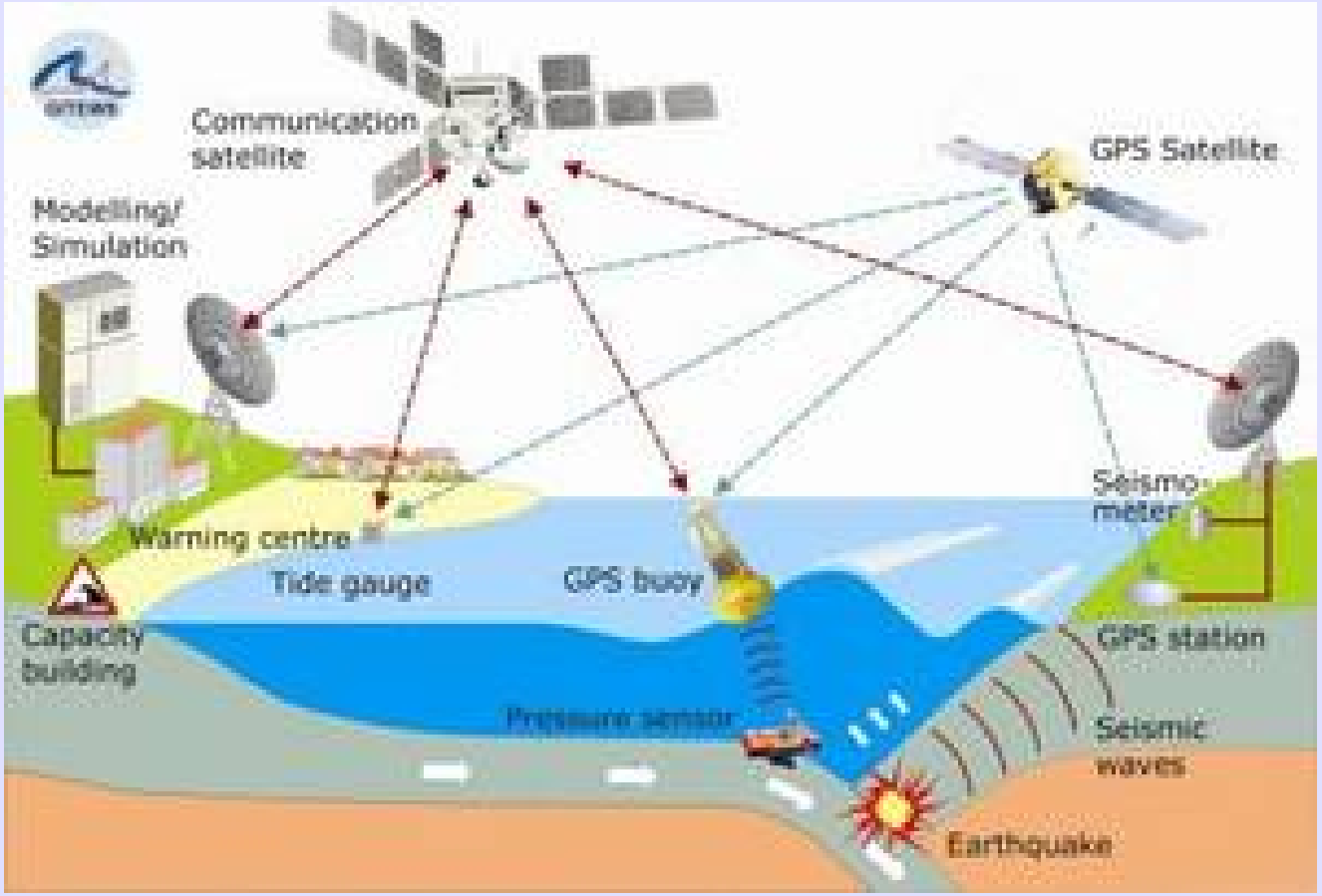

http://www.gitews.de/

Fig. 11 The HF radar WERA (Wellen Radar) system installation

(a) the transmitting array

(b) the receiving array

(A. Dzvonkovskaya et al., European Journal of Navigation, vol. 7, No. 2, 17-23, 1 Aug. 2009)

Fig. 12 Example of measured range-Doppler power spectrum

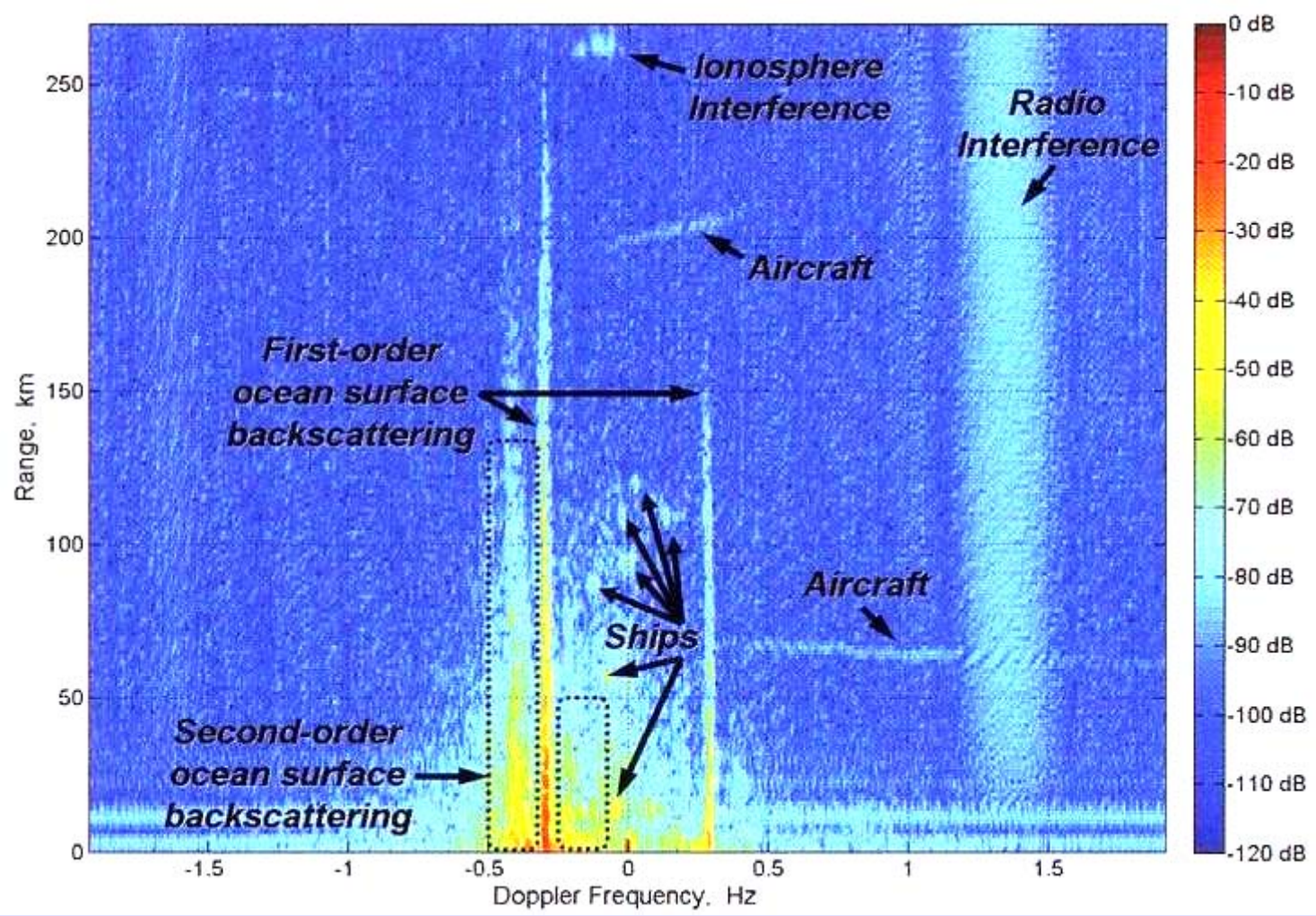

(A. Dzvonkovskaya et al.,European Journal of Navigation, vol. 7, No. 2, 17-23, 1 Aug. 2009)

Fig. 13 Simulated tsunami-induced current velocity by HAMSOM

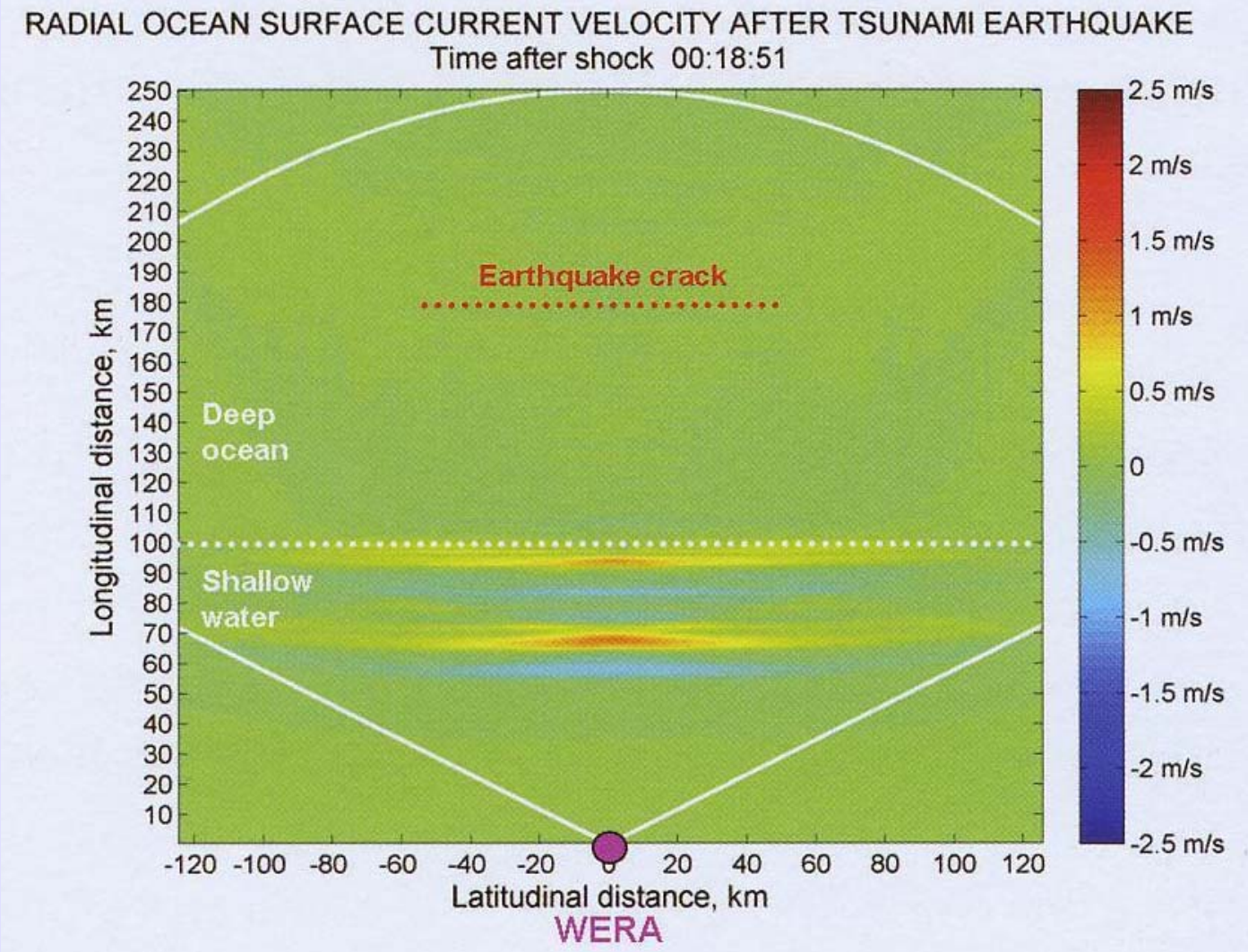

HAMSOM: Hamburg Shelf Ocean Model

(A. Dzvonkovskaya et al.,European Journal of Navigation, vol. 7, No. 2, 17-23, 1 Aug. 2009)

Fig. 14 Measured spectrum

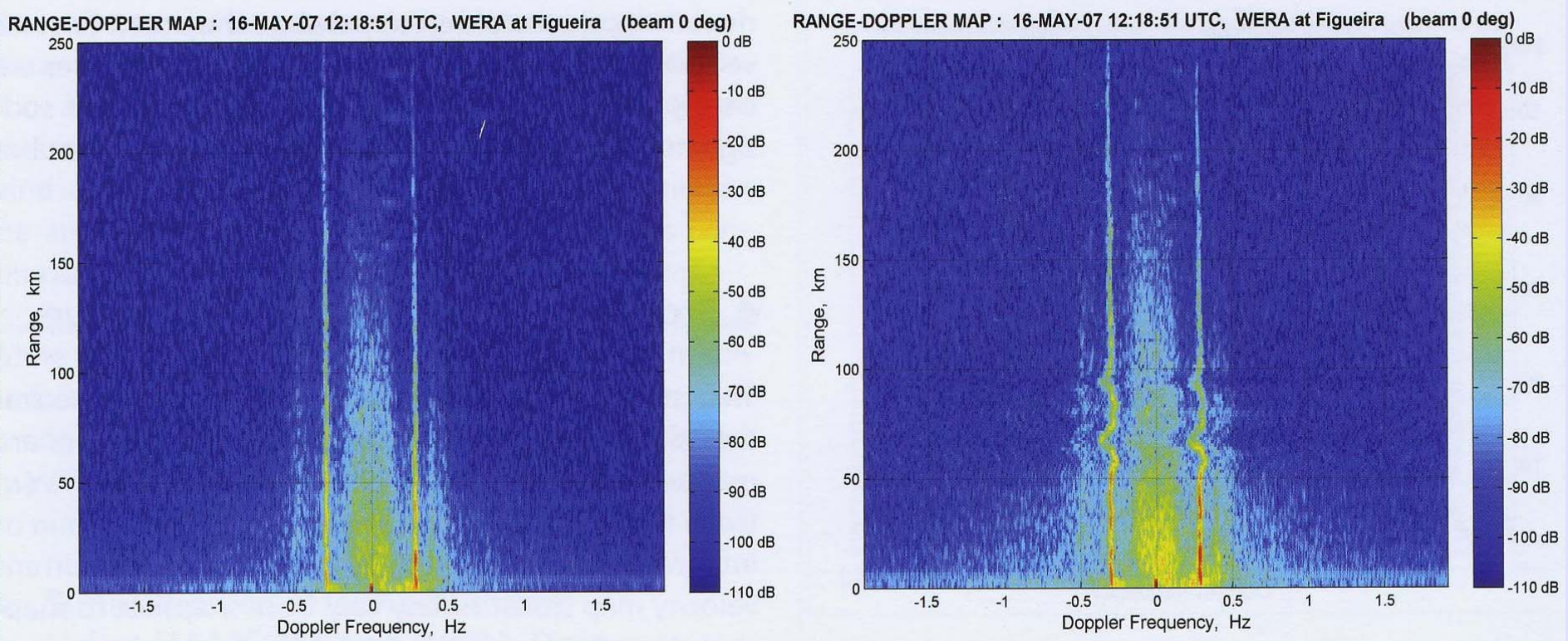

without tsunami.

superimposed with tsunami currents
(19min after the earthquake)

(A. Dzvonkovskaya et al.,European Journal of Navigation, vol. 7, No. 2, 17-23, 1 Aug. 2009)

Fig. 15 Map of radial ocean surface current velocity of Fig. 13

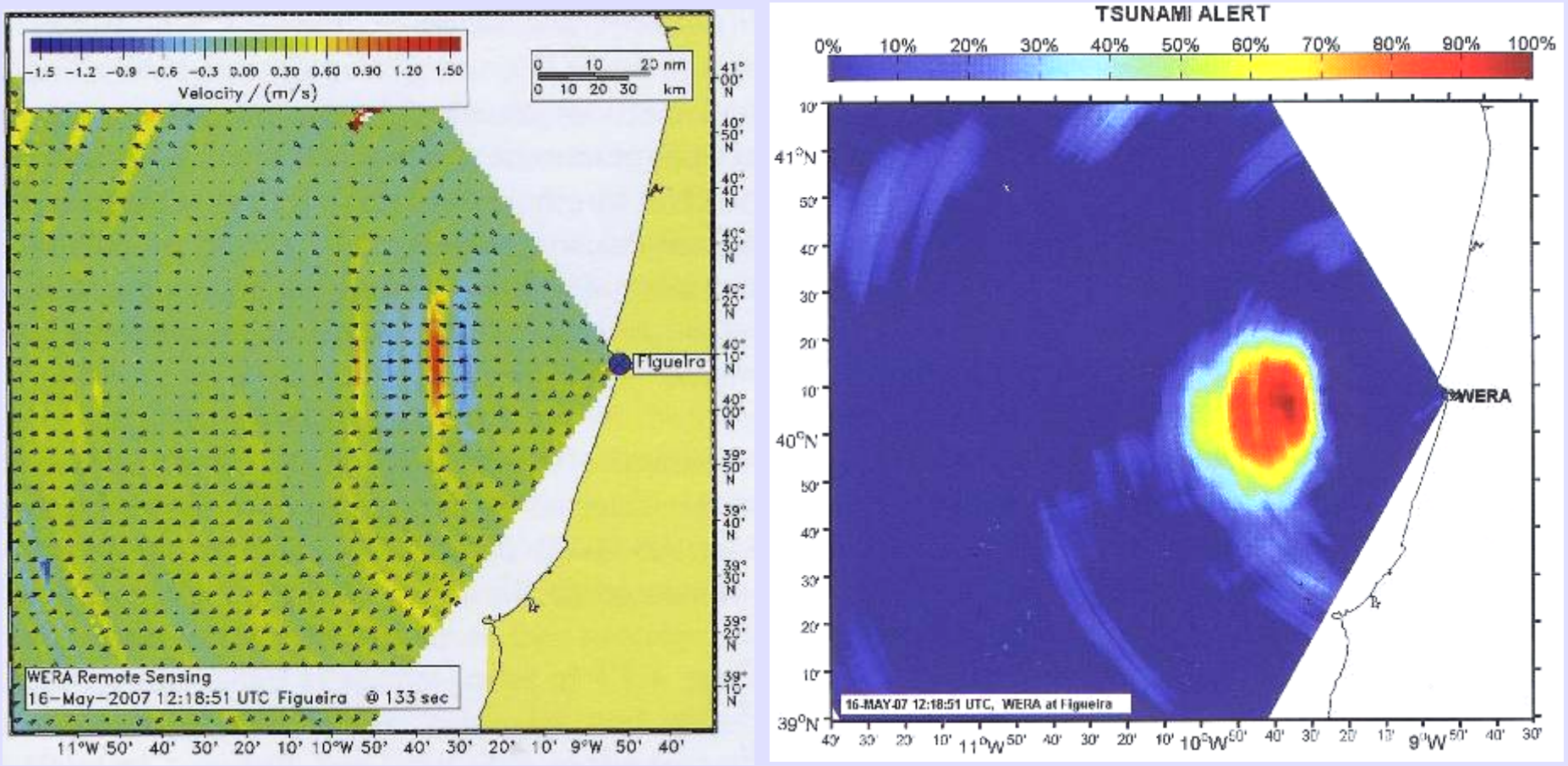

(A. Dzvonkovskaya et al.,European Journal of Navigation, vol. 7, No. 2, 17-23, 1 Aug. 2009)

Fig. 16 Japan (East Coast of Honshu) tsunami, March 11, 2011

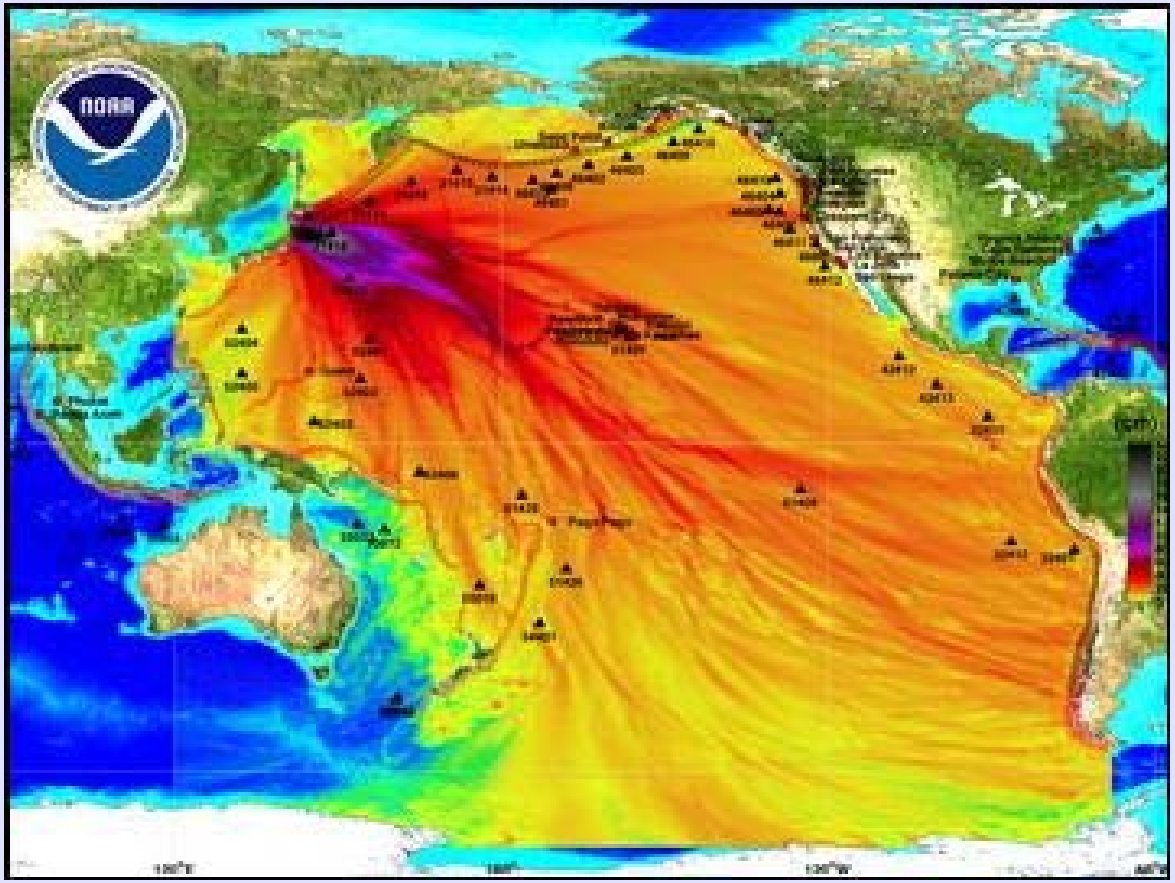

http://nctr.pmel.noaa.gov/

Fig. 17 WERA ocean radar system at Rumena, Chile

The system operates at 22MHz and consists of a short array of 8 antennas that receives the backscattered signal.

HELZEL Messtechnik

http://www.helzel.com/

Fig. 18

Current velocities as function of time and range

Tide gauge measurement at 50km.

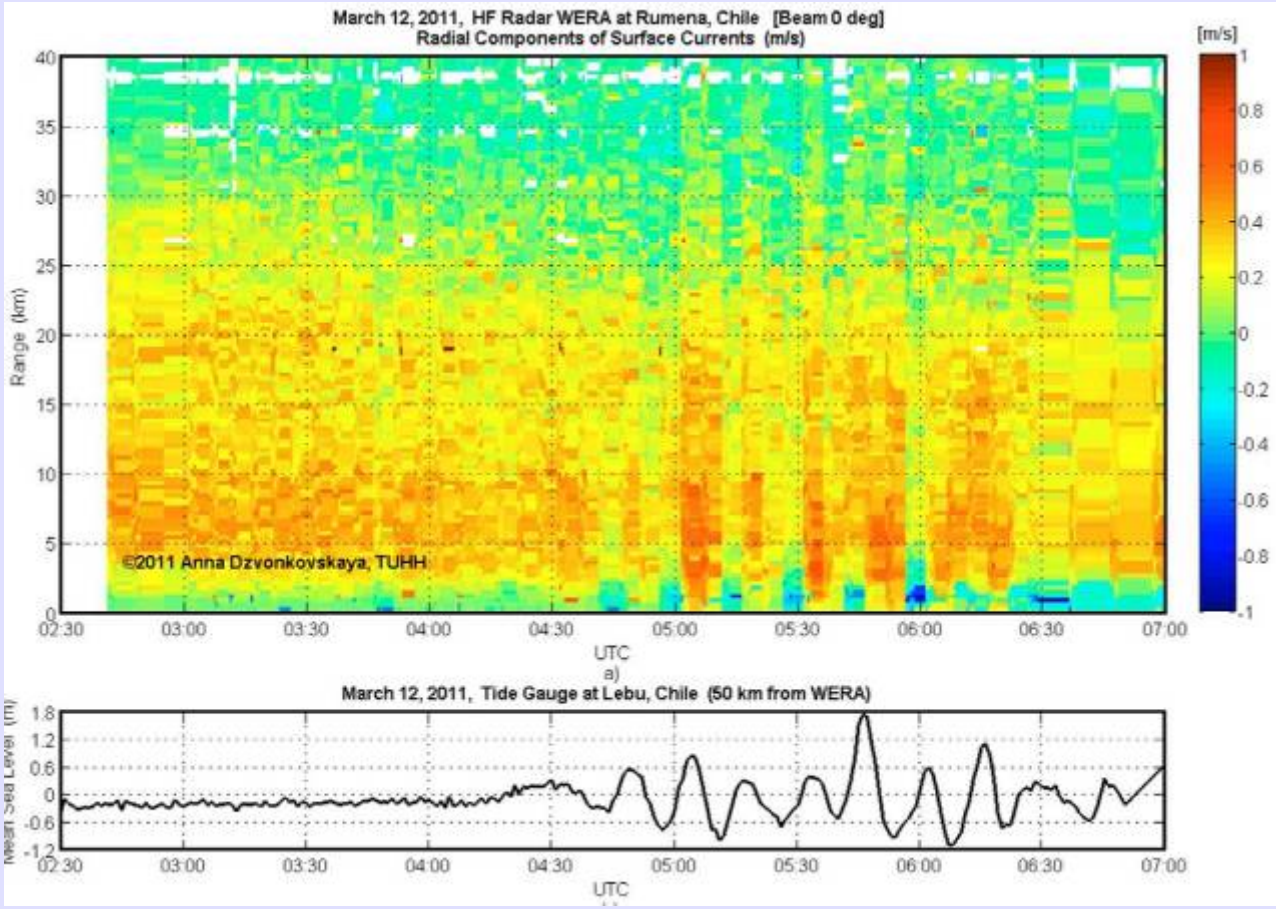

Barrick, Lipa等の東北太平洋沖津波探知の研究発表

1 Remote Sensing, 2011, 3, 1663-1679
Belinda Lipa, Donald Barrick, Sei-Ichi Satoh, Yoichi Ishikawa, Toshiyuki Awaji, John Largier, and Newell Garfield,
“Japan tsunami current flows observed by HF radars on two continents.”

2 IEEE Ocean-2011, September Hawaii.
Donald Barrick and Belinda Lipa,
“Japan tsunami detected by HF radars on two continents.”

Figure 1. (a) The North Pacific Ocean showing the location of the radars in Japan and California that provided data for this paper; **(b)** The location of the Japan earthquake and the radars in Hokkaido; **(c)** The bathymetry offshore from the radars and radial velocities measured by the Kinaoshi radar, 11 March 2011, 21:00 JST.

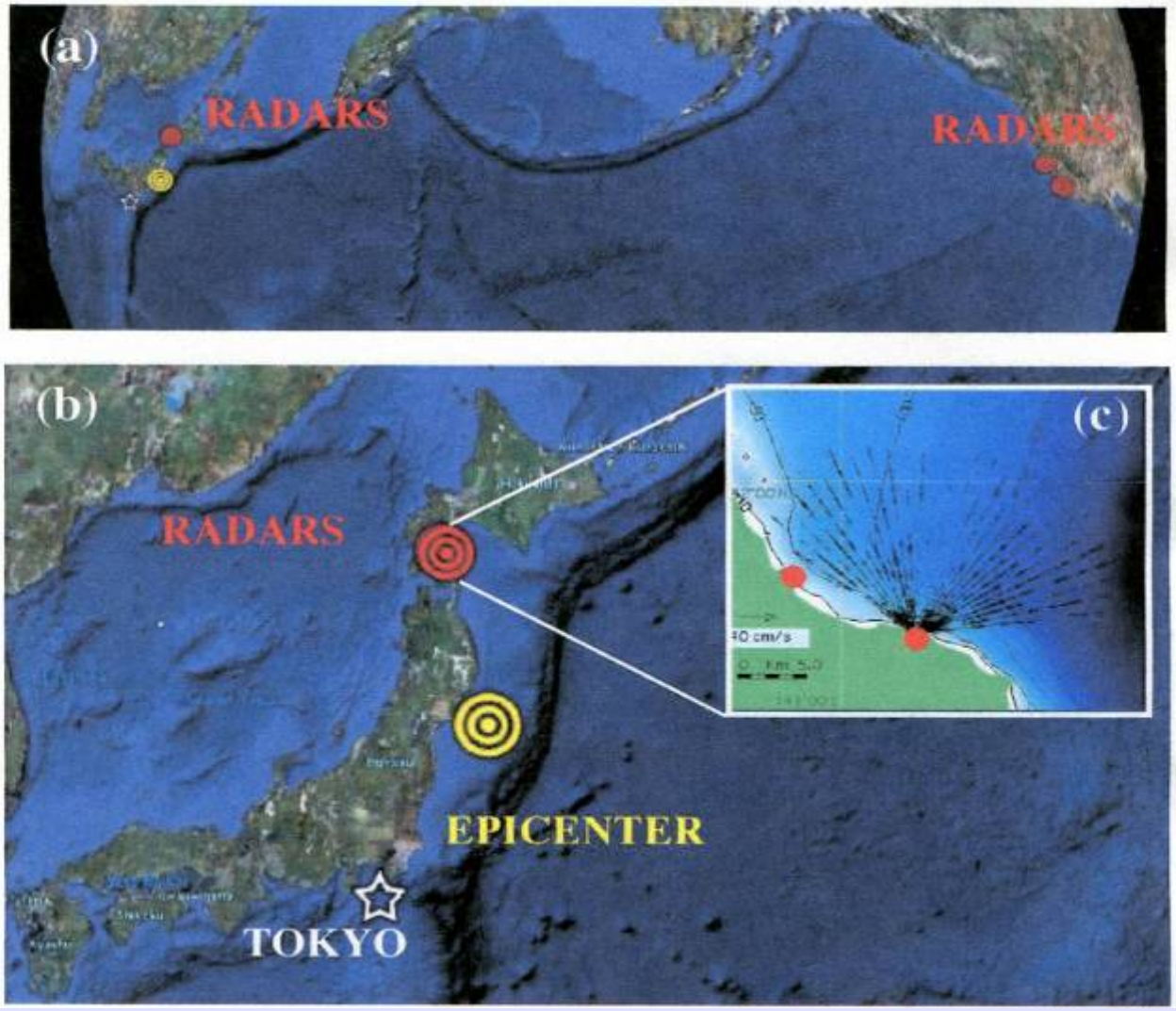

Figure 2. The tsunami height superimposed on the total current velocity field measured by radars at Usujiri (blue dot) and Kinaoshi (red dot): **(a)** 11 March 2011, 15:53 JST; **(b)** 11 March 2011, 21:00 JST.

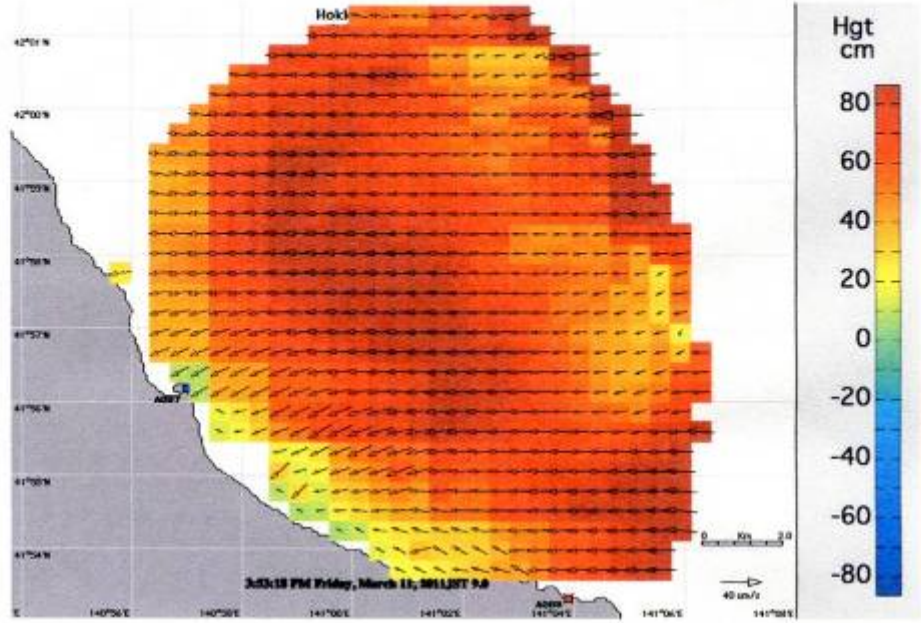

(a)

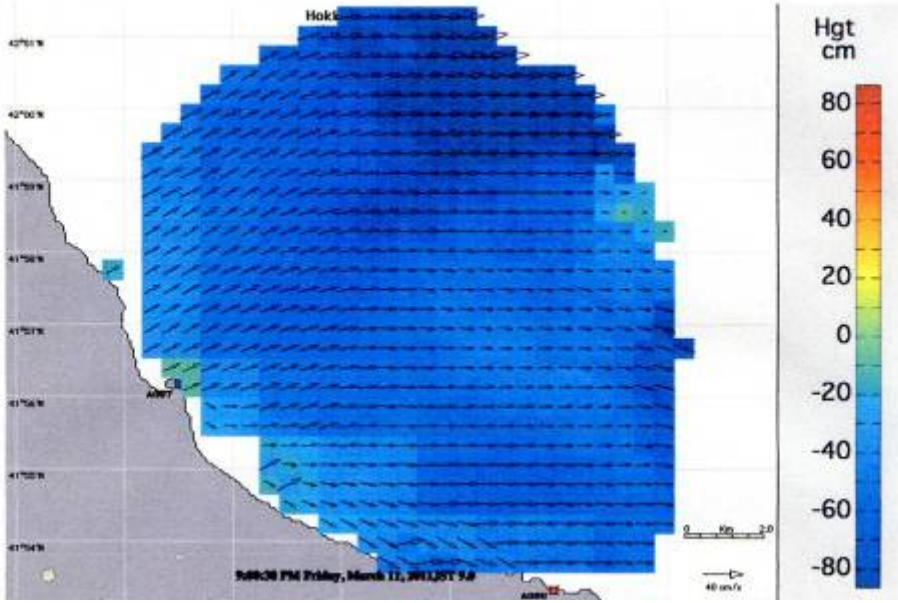

Figure 5. The location of the radar at the Bodega Marine Lab., California, the offshore bathymetry and a measured radial velocity map. Measured radial velocities are for 11 March 2011, 16:52 UTC, and show the reverse flow generated by the tsunami in the inner range calls.

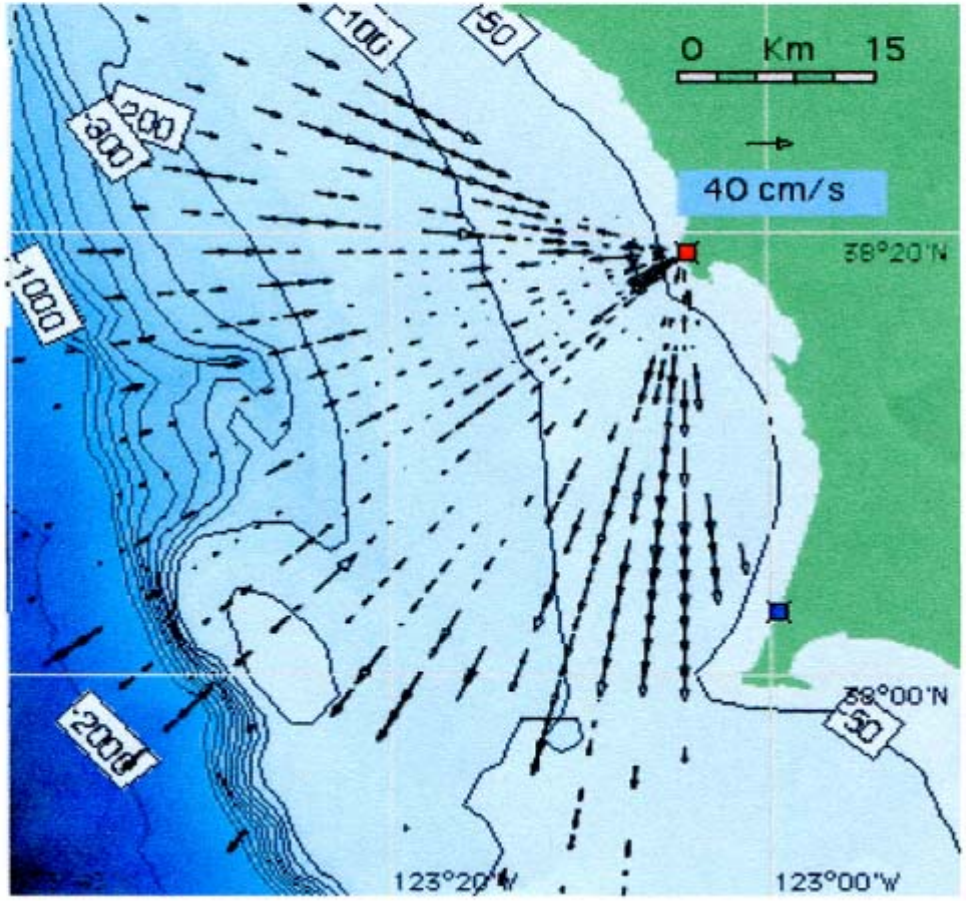

おわりに

2004年 マイクロ波帯電波高度計がdeep oceanの津波を明瞭に探知　波高のプロファイルとtsunami shadows

2011年 HFレーダがcoastの津波を明瞭に探知
surface currentのDoppler signature

レーダは津波の研究及び早期探知警戒のための有力なツール
地球物理学や海洋工学等の科学技術知識とのシナジー

今後の期待
中小の津波, 様々な気象海象下で有効なレーダ
未開拓のsignature